Electrospun Azo-Cellulose Fabric: A Smart Polysaccharidic Photo-Actuator

Hamed Ahmadi-nohadani, Steve Nono-tagne, Christopher Barrett, Issei Otsuka

PREPRINT

(Original article published in Macromol. Rapid Commun. 2022, 43(9), 2200063 by Wiley-VCH Verlag, DOI: 10.1002/marc.202200063)

Electrospun Azo-Cellulose Fabric: A Smart Polysaccharidic Photo-actuator

*Hamed Ahmadi-Nohadani, Steve Nono-Tagne, Christopher J. Barrett, and Issei Otsuka**

H. Ahmadi-Nohadani, S. Nono-Tagne, I. Otsuka
Université Grenoble Alpes, CNRS, CERMAV, Grenoble 38000, France
E-mail: issei.otsuka@cermav.cnrs.fr

C. J. Barrett
Department of Chemistry, McGill University, Montreal H3A 0B8, Canada

Keywords: cellulose, azobenzene, electrospinning, nonwoven fabrics, photo-actuators

ABSTRACT: A natural polysaccharide-based smart photo-actuator is fabricated via electrospinning of cellulose 4-phenyl azobenzoate (Azo-Cel) from its organic solution in a mixture of high-volatile acetone, a poor solvent of Azo-Cel, and low-volatile *N*,*N*-dimethylacetamide (DMAc), a good solvent of Azo-Cel. At an optimal polymer concentration (17 wt%) and solvent mixing ratio (acetone/DMAc = 3/2 (v/v)), stable electrified polymer jets are formed and continuous nanofibers and their nonwoven fabric can be drawn on a cylinder-shaped rotating drum electrode under a high electric field (25 kV). Scanning electron microscopic observation of the Azo-Cel fabric confirms that the fabric consists of uniaxially-aligned nanofibers with a mean diameter of 207 nm. The water contact angle of the Azo-Cel fabric reversibly decreases and increases in response to alternate irradiation with UV and visible light to induce geometric deformation of the azobenzene moiety between the *trans* and *cis* isomers, which lead to lower and higher surface free energies, respectively. In addition, self-standing Azo-Cel fabric exhibits a UV-driven photo-mechanical asymmetric bending deformation toward the light source.

1. Introduction

There has recently been a great and timely increase in demand for nonwoven fabrics that are a key component of disposable face masks, for example, due to epidemic infectious diseases such as COVID-19.[1] This has focused more recent attention to electrospinning,[2-5] a well-established method of nanofibrous textile fabrication. The high specific surface area of electrospun nanofibrous textiles arising from the nanoscale interstitial spaces between the nanofibers makes them a promising scaffold to filter micro-scale biological and chemical contaminants. In addition to this effect of nano-size structure, a very important characteristic of the electrospun fabrics is that their morphology (e.g., the diameter and orientation of the fibers) can be controlled simply by adjusting technical electrospinning parameters such as solvent, concentration, solution feed rate, electric field, etc. and by using special electrodes (e.g., a program-moving rotative electrode). Thanks to this feature, electrospun fabrics possessing superior mechanical resistance, *i.e.*, high tensile strength and Young's modulus, have been obtained by optimizing the diameter of the fibers and aligning them in desirable directions.[6-8] Currently, raw materials of electrospun fabrics include bio-based polymers and are not limited to fossil fuel-based polymers,[9-10] and electrospun fabrics made of polysaccharides and their derivatives are one of the most rapidly-growing product markets for various biomedical applications such as drug delivery, tissue engineering, wound healing, biosensors, etc.[11-13] In addition, polysaccharides, notably cellulose, can offer robust scaffolds of smart materials thanks to their inherently superior mechanical properties.[14-18] In this context, we are developing new types of smart cellulosic fabrics via electrospinning, aimed at diverse applications including membrane filters for efficient resolution of biologically essential chiral molecules,[19] as well as photo-responsive materials,[20] that are the main targets of this study.

Among various stimuli-responses of photo-responsive materials,[21-23] special attention has been paid to their light-driven deformation. This photo-actuation behavior can be precisely

and remotely controlled without any physical connections such as electrical cables that are necessary for other types of actuation, for instance, with piezoelectrics. Azobenzene-containing polymeric materials[24-26] have been widely studied for their photo-actuation behavior that originates from the nanoscale *cis*/*trans* geometric photo-isomerizations of the azobenzene moiety, that can be amplified cooperatively to induce macroscopic deformations of the materials. Notably, liquid crystal polymers (LCPs) containing azobenzene derivatives as their mesogenic pendant groups have demonstrated fast stimuli-response speeds and large deformation extents, which are enhanced by the cooperative nature of liquid crystal ordering.[27-32] In principle, the *trans* isomer of azobenzene having a rod-like shape stabilizes the structure of liquid crystal phase, while the *cis* isomer having a bent-shape tends to destabilize the phase. Recently, photo-actuation of non-liquid-crystalline polymers containing azobenzene under specific conditions has been also reported.[33-35] Although these azobenzene-containing polymers possess great photo-deformable effects in the form of their crosslinked or networked gels or films, there are some fundamental drawbacks for practical applications such as artificial muscles in soft robotics because of their weak mechanical strength and thermal resistance. Therefore, designing polymeric photo-actuators in other forms than gels or films is of great importance. Our approach to tackle this challenging task is the electrospinning of a photo-responsive cellulose 4-phenyl azobenzoate (Azo-Cel) to form robust and flexible photo-responsive fabrics.

Previously, we reported the synthesis, the *cis*/*trans* geometric photo-isomerizations of the azobenzene moiety, and the electrospinnability (under specific conditions) of Azo-Cel as a proof of concept for a new type of photo-actuator.[20] In this study, the electrospinning conditions of Azo-Cel are optimized to form a strong self-standing fabric that exhibits both light-driven wettability changes and asymmetric photo-mechanical bending deformations.

2. Results and Discussion

2.1. Optimization of the Electrospinning Conditions

Previously, we reported the synthesis of Azo-Cel, its photo-responsive properties in solution, and a preliminary exploration of its successful electrospinning.[20] In the previous study, we found that a mixture of high-volatile and low-volatile good solvents at a certain ratio, i.e., a mixture of dichloromethane (DCM: boiling point (bp) = 39.6 °C, vapor pressure (vp) = 47.1 kPa at 20 °C) and *N*,*N*-dimethylformamide (DMF: bp = 153 °C, vp = 0.516 kPa at 20 °C) with the volume ratio of DCM/DMF = 3/1, provided a stable electrospinning process of Azo-Cel to form continuous nanofibers when the polymer concentration was fixed to 10 wt%. However, this solvent system was not optimal for longer duration electrospinning processes to from self-standing thick fabrics, because the polymer solution tended to agglomerate on the tip of the needle electrodes and impeded the polymer feed. Therefore, we explored other solvent systems to avoid this problem. Interestingly, mixing high-volatile poor solvents with low-volatile good solvents successfully prevented the agglomeration of Azo-Cel on the tip of the needle electrodes. Among various combination of the solvents, a mixture of high-volatile acetone (bp = 56.0 °C, vp = 30.0 kPa at 20 °C), a poor solvent of Azo-Cel, and a low-volatile *N*,*N*-Dimethylacetamide (DMAc: bp = 165 °C, vp = 0.33 kPa at 20 °C), a good solvent of Azo-Cel, provided a consistently stable electrospinning process without agglomeration. Figure 1 presents Scanning Electron Microscopy (SEM) images of the electrospun products from Azo-Cel solutions in the mixture of acetone and DMAc with volume ratios of acetone/DMAc = 1/1 and 3/2 and concentrations 13, 15, and 17 wt%. As presented in Figures 1a and 1d, the electrospun products from the 13 wt% solutions displayed spherical bead-like structures regardless of their solvent volume ratios, probably because the viscosities and/or the surface tensions of the polymer solutions were insufficient against the applied electrostatic force so that the polymer solutions quickly sprayed away from the tip of the needle in the form of spherical droplets. By increasing

the concentration to 15 wt %, a number of fibers coexisting with spherical beads were formed as shown in Figures 1b and 1e. One notes that increasing the volume ratio of acetone/DMAc from 1/1 to 3/2 tended to suppress the formation of spherical beads. A further increase of the concentration to 17 wt% (above this concentration, the polymer solution coagulates) fostered the formation of continuous fibers as presented in Figures 1c and 1f. Consequently, we chose acetone/DMAc = 3/2 (v/v) and 17 wt% as the optimal condition for the preparation of the self-standing Azo-Cel fabric.

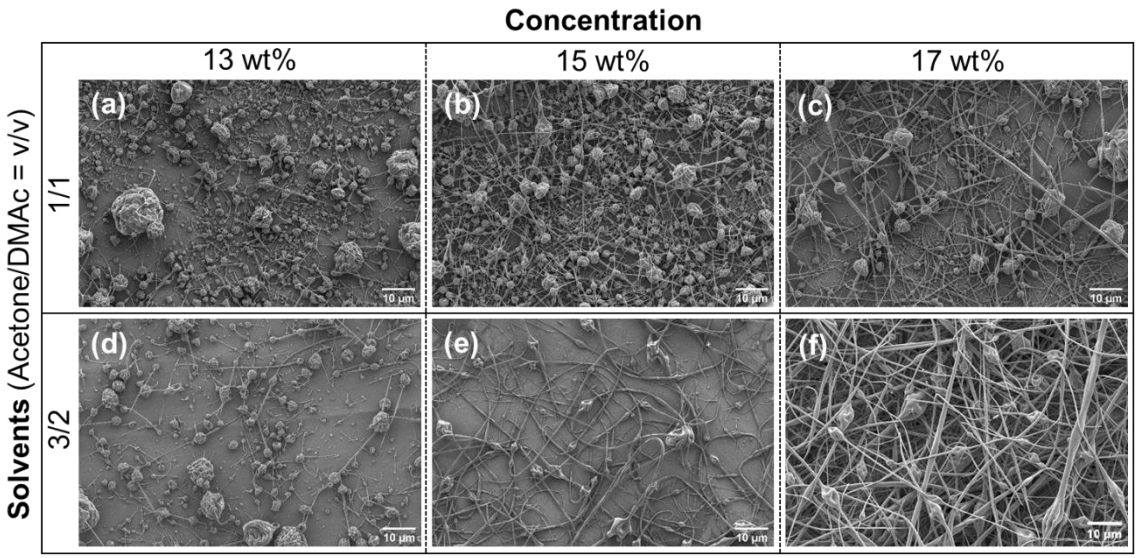

Figure 1. SEM images of the electrospun products obtained from the Azo-Cel solutions in mixtures of acetone and DMAc with different volume ratios and concentrations: the products from (upper row) acetone/DMAc = 1/1 (v/v) solutions with (a) 13 wt%, (b), 15 wt%, and (c) 17 wt%, and (lower row) acetone/DMAc = 3/2 (v/v) solutions with (d) 13 wt%, (e), 15 wt%, and (f) 17 wt%.

2.2. Preparation of Self-standing Azo-Cel Fabric

Previous studies revealed that alignment of electrospun fibers in a uniaxial direction improves the mechanical properties of the resulting fabrics, including the tensile strength along the

principal fiber axis and the Young's modulus, compared to non-aligned fibrous fabrics.[6-8, 36] Therefore, in this study, we employed a cylinder-shaped rotating drum electrode as a collector of the electrospun textile to fabricate an uniaxially-aligned nanofibrous Azo-Cel fabric. One of the key steps to obtain self-standing fabrics via electrospinning is the process of detaching the textile from the substrate (aluminum (Al) foil in most cases). A preliminary test of electrospinning Azo-Cel directly on an Al foil showed that the resulting Azo-Cel textile strongly adheres to the Al foil, making it difficult to detach the textile without damaging it. To avoid this technical problem, a water soluble polymer, polyethylene oxide (PEO), was first electrospun on an Al foil followed by Azo-Cel to prepare a double-layered "Azo-Cel on PEO" textile on the Al foil. As Azo-Cel is not soluble in water, this double-layered textile on the Al foil was immersed in water to selectively solubilize the PEO layer that serves as a form of adhesion promotion layer between the Al foil and the Azo-Cel textile. In this way, the Azo-Cel layer was successfully detached from the Al foil without damage as a floating textile on the water. The obtained self-standing Azo-Cel fabric was dried in vacuo and used for the following physical property analyses: Firstly, Figure 2 presents Attenuated Total Reflection-Fourier Transform Infrared (ATR-FTIR) spectra of the self-standing Azo-Cel fabric and the PEO textile for comparison. In the spectrum of the self-standing Azo-Cel fabric (Figure 2a), a characteristic absorption band of the C-H stretching vibrations in the PEO backbone observed around 2880 cm^{-1} in Figure 2b disappeared, indicating a successful elimination of the PEO layer in the fabric. Secondly, Figure 3 shows a SEM image of the self-standing Azo-Cel fabric and a histogram of the constituent fiber diameter distribution. As presented, the self-standing Azo-Cel fabric consisted of almost uniaxially-aligned nanofibers with the mean diameter of 207 nm.

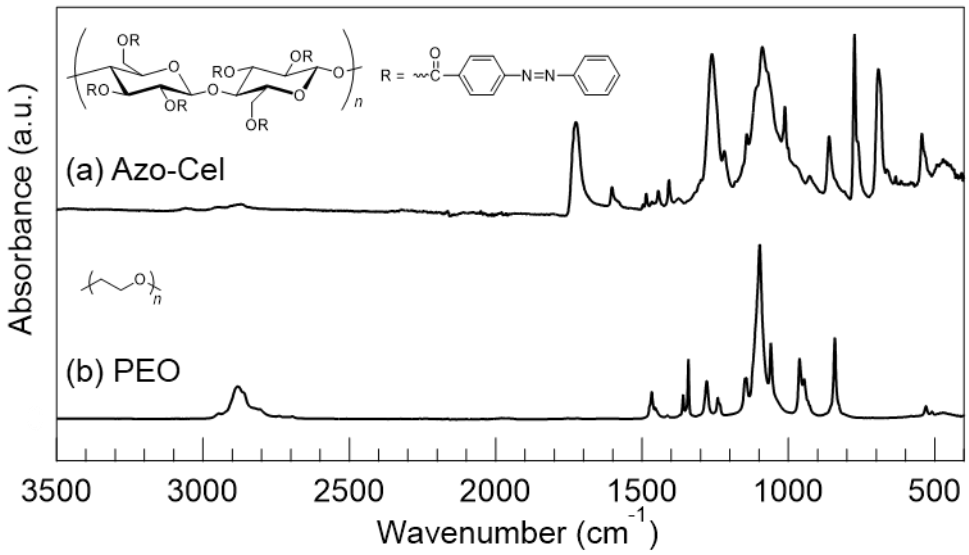

Figure 2. ATR-FTIR spectra of (a) the self-standing Azo-Cel fabric and (b) the PEO textile.

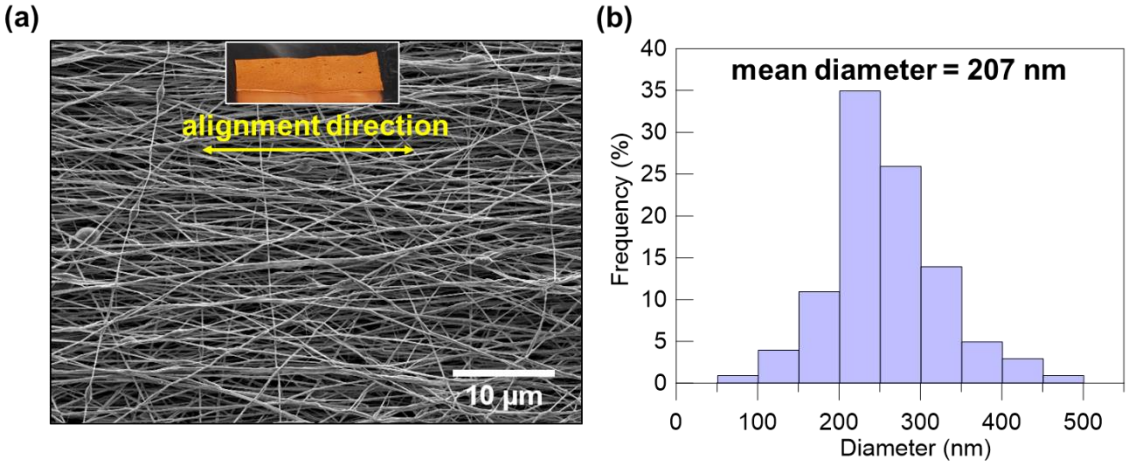

Figure 3. (a) A SEM image of the self-standing Azo-Cel fabric (an inserted photo) and (b) a histogram of the diameter distribution of the fibers in the fabric determined from the SEM image by ImageJ open-source software.

2.3. Light-driven Wettability Changes on the Azo-Cel Fabric

Under light irradiation, photo-responsive materials can change their molecular geometric structures, which is frequently accompanied by variations of molecular polarity and surface free energy, leading to an induced transition of surface wettability.[37] In the case of azobenzene-functionalized materials, photo-isomerization of the azobenzene moiety between its *trans* and *cis* isomers causes a change in dipole moment, resulting in a change of surface wettability. The *trans* isomer with a smaller dipole moment has a lower surface free energy, and the *cis* isomer with a larger dipole moment has a higher surface free energy.[38-39] Therefore, the materials having the *trans* isomer generally show greater Water Contact Angle (WCA) than those having the *cis* isomer.[40-41] A similar phenomenon was observed for the Azo-Cel fabric. One notes that the photo-isomerization of the azobenzene moiety in Azo-Cel from the *trans* to the *cis* isomers under UV irradiation and vice versa under visible light irradiation in the solution state was reported in our previous study.[20] A WCA of an Azo-Cel fabric was first measured as it was obtained (a picture of a water droplet on the as-spun Azo-Cel fabric is shown in Figure 4a), then the same Azo-Cel fabric was irradiated with UV for 15 min followed by its WCA measurement (Figure 4b). The specimen was left for 30 min under visible light before measuring its WCA again (Figure 4c). The above-mentioned procedure was repeated for 5 cycles and variation of the WCA was plotted in Figure 4d, where the WCA values are the mean values of 4 sets of the measurements using different pieces of Azo-Cel fabric, and the error bars represent their maximum and minimum values. It should be noted that the small hysteresis and range of the WCA values are probably due to rough surfaces of the Azo-Cel fabric because the surface nano/microstructure is one of the important factors of the surface wettability. As presented in the Figure 4d, the WCA was reversibly changed by the UV and visible light irradiations (averaged angle change was 8.7°), indicating that the photo-isomerization of the azobenzene moiety in the Azo-Cel fabric induced the changes of its surface wettability.

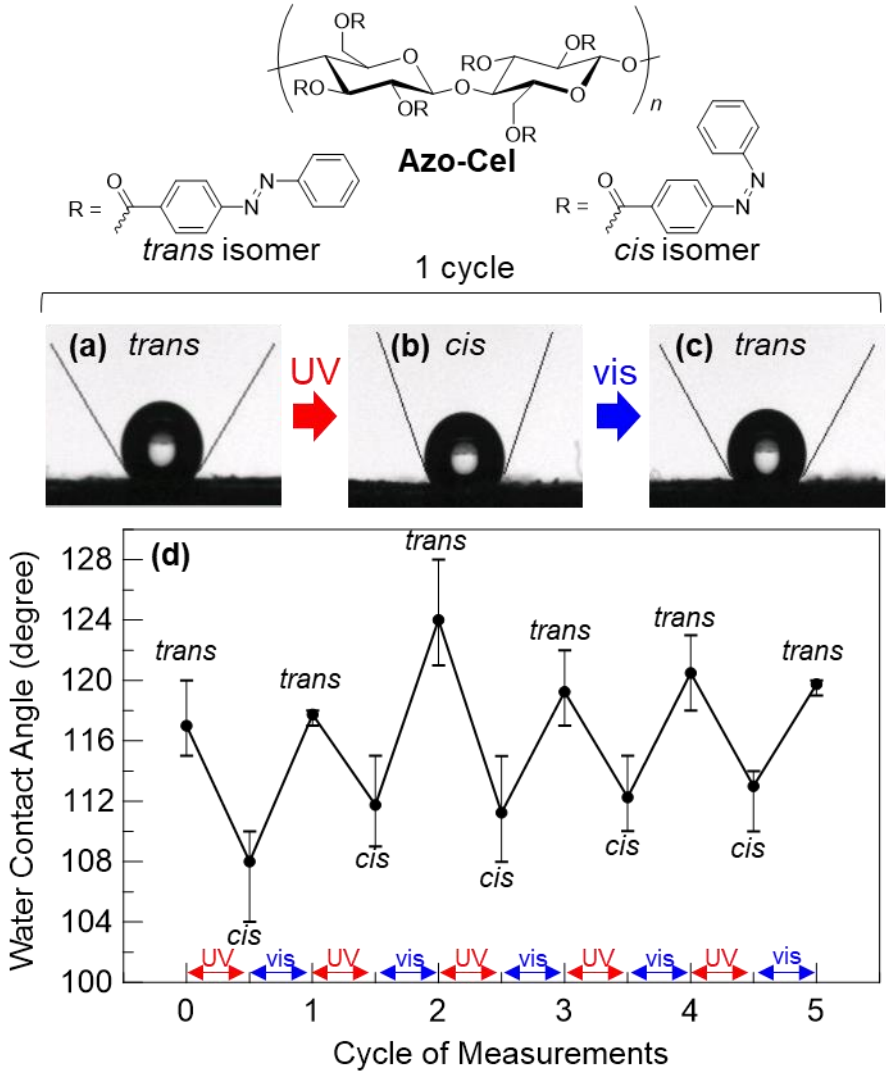

Figure 4. Photos of water droplets on (a) an as-spun Azo-Cel fabric (*trans* isomer): WCA = 120°, (b) the same fabric after UV radiation (*cis* isomer): WCA = 108° and (c) the same fabric after visible light irradiation (*trans* isomer): WCA = 118°. (d) The WCA changes of the Azo-Cel fabric over 5 cycles of UV/visible light irradiations. The plotted WCA values are the mean values of 4 sets of the measurements using 4 different pieces of the Azo-Cel fabric, and the error bars represent their maximum and minimum values.

2.4. Photo-actuation of the Azo-Cel Fabric

Many of the azobenzene-functionalized materials that have been reported have the potential to convert photo-stimuli into mechanical deformations, in other words, a photo-actuation

property.[26] Among them, a pioneering work of UV-driven azo material bending toward the light source was reported by Ikeda et al. on azobenzene-functionalized LCP films.[27] The key of this asymmetric bending deformation of the film was that the photo-isomerization from the rod-like *trans* isomer to the bent-shape *cis* isomer of the azobenzene moiety occurred only in the surface region of the film facing the UV light source, but not in the bulk of the film because most of the incident photons are absorbed near the surface, within a thickness of less than 1 μm due to the large molar extinction coefficient of the azobenzene moiety (2.6×10^4 L mol^{-1} cm^{-1}). The resulting gradient distributions of the bent-shape *cis* isomers in the thickness direction of the film led to a stress gradient, which induced the bending of the film toward the light source. We here observed a similar UV-driven asymmetric bending deformation of the Azo-Cel fabric toward the light source (Figure 5). Figure 5b shows a series of photographs of a piece of the Azo-Cel fabric placed 2 cm away from the UV light source (at the left-side in the photos) over the time of irradiation with light intensity = 45 mW cm^{-2}. As presented in the figure, the Azo-Cel fabric clearly bent toward the UV light source over time, and the bending angle from the initial state became about 15° after a 30 min irradiation. As a control experiment, an electrospun fabric made of cellulose acetate (CA), which consists of the same cellulosic backbone as Azo-Cel yet a non-photo-responsive acetyl group as the pendant group, was irradiated by UV under the same conditions (Figure 5d). In stark contrast to the Azo-Cel fabric, the CA fabric did not bend at all under the UV irradiation, suggesting that the bending deformation of the Azo-Cel fabric was induced by the photo-isomerzation of the azobenzene moiety in the Azo-Cel. One notes that co-electrospinning of CA with free azobenzene did not produce homogeneous fibrous fabrics because the CA and the azobenzene molecules were phase separated during the spinning process and formed huge aggregates of azobenzene in the CA fabric as shown in Figure S2 (see supporting information). Therefore, chemical modification of cellulose with azobenzene groups is confirmed essential to electrospin such a photo-responsive cellulosic fabric.

UV irradiation of the Azo-Cel fabric from longer and shorter distances also supports the UV-driven bending mechanism. Figures 5a and 5d respectively present bending behaviors over time of 2 pieces of the Azo-Cel fabric placed at 4 cm (25 mW cm^{-2}) and 1 cm (60 mW cm^{-2}) away from the light source. As can be seen in Figure 5a, the UV irradiation from a longer distance (4 cm) barely bent the Azo-Cel fabric, and the bending angle after 30 min irradiation was not clearly detected, while that observed at a medium distance (2 cm) shown in Figure 5b was evident. This can be explained by the lower light intensity (25 mW cm^{-2}) from the longer distance not being sufficient to photo-isomerize the azobenzene moiety in the surface region of the Azo-Cel fabric from the *trans* to the *cis* isomers, which must be the driving force of the asymmetric bending. On the other hand, the UV irradiation from a shorter distance (1 cm) clearly induced an asymmetric bending of the Azo-Cel fabric toward the light source, while the bending angle (ca. 10°) was smaller than that observed in the Azo-Cel fabric irradiated from the medium distance (ca. 15°) shown in Figure 5b. Such a decrease of the bending angle (-5°) was possibly due to deeper penetration of photons from the shorter distance (1 cm) with higher light intensity (60 mW cm^{-2}) compared to those from the medium distance (2 cm) with medium light intensity (45 mW cm^{-2}), which decreases the gradient distributions of the *cis* isomers in the thickness direction of the fabric, and thereby leads to the less asymmetric deformation (i.e., smaller bending angle). Such intermediate irradiation optimization conditions have been observed previously for azo photo-mechanical materials,[25] balancing higher driving input power, with confinement to the near-surface region only. At optimal irradiation conditions however, the Azo-Cel fabric clearly demonstrated strong photo-actuation behavior. To put this novel polysaccharidic photo-actuator to practical use, for instance as an artificial muscle, photo-deformable performance parameters such as stimuli-response speed, and deformation extent, still must be improved. Previous studies on azobenzene-functionalized materials have shown that regularly aligned azobenzene units can cooperatively amplify nanoscopic geometric

variations of an individual azobenzene molecule into macroscopic deformations. Therefore, further studies on structural ordering of azobenzene moieties in Azo-Cel by regioselective functionalizations of cellulose and thermal annealing of the fabric are under investigation with a view to optimize crystallinity of the Azo-Cel fabric to obtain better photo-deformable performance and mechanical properties.

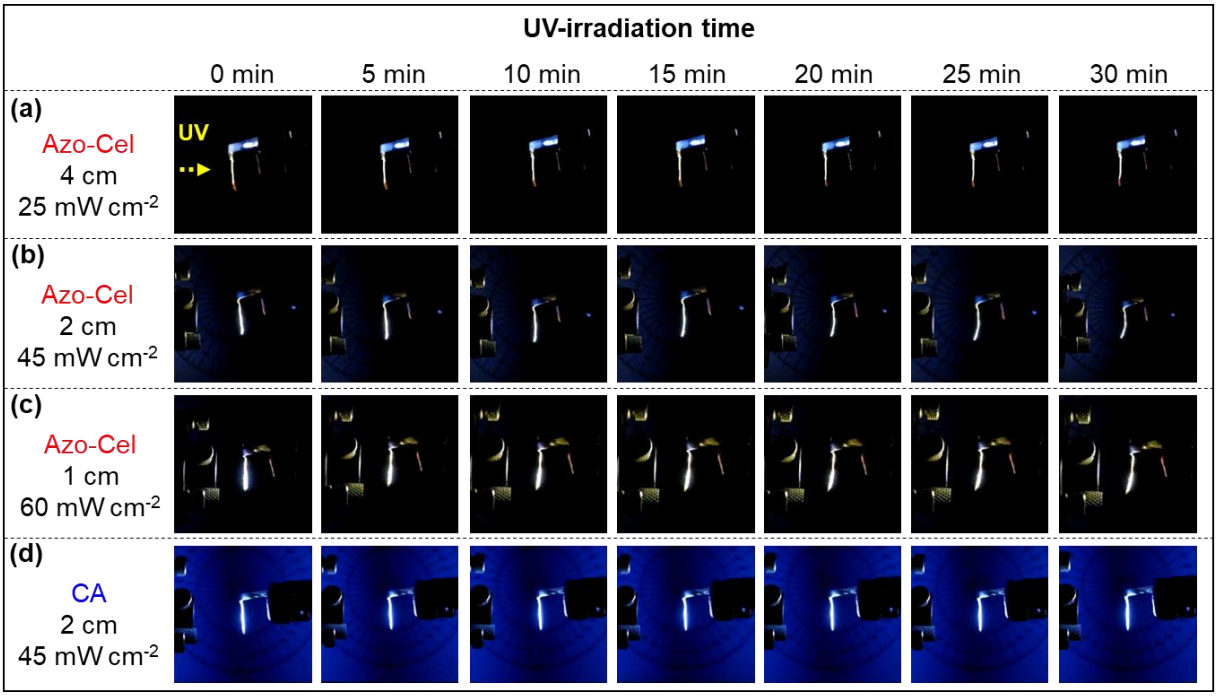

Figure 5. Series of pictures of Azo-Cel and CA fabrics irradiated by UV over time of the irradiation: (a) Azo-Cel placed at 4 cm away (the light intensity = 25 mW cm^{-2}), (b) Azo-Cel placed at 2 cm away (45 mW cm^{-2}), (c) Azo-Cel placed at 1 cm away (60 mW cm^{-2}), and (d) CA placed at 2 cm away (45 mW cm^{-2}) from the UV light source (at the left-side in the pictures).

3. Conclusions

The electrospinning process of Azo-Cel was stabilized by using a mixed solvent consisting of a high-volatile poor solvent: acetone, and the low-volatile good solvent: DMAc, with an optimal volume ratio and concentration, and using a rotating drum collector to form the self-standing

Azo-Cel fabric consisting of uniaxially-aligned nanofibers. The Azo-Cel fabric demonstrated clear photo-responsive properties, i.e., (i) the light-driven wettability changes supported by the photo-isomerization of the less polar *trans* isomer to the more polar *cis* isomer under UV light and vice versa under visible light, and (ii) the UV-driven actuation behavior observed as the asymmetric bending deformation toward a light source. Although the photo-deformable performances must be further ameliorated, such smart polysaccharidic fabrics have a great potential for practical applications as novel photo-actuators.

4. Experimental Section

Materials: Microcrystalline cellulose (MCC: Avicel PH-105; derived from wood pulp; ~20 μm particle size) was purchased from FMC BioPolymer Co. and vacuum dried for 24 h at 60 °C prior to use. 4-(Phenylazo)benzoyl chloride (≥ 98.0%) was purchased from Tokyo Chemical Industry Co. and used as received. Cellulose acetate (CA: $M_n \approx 30{,}000$; calculated DS ≈ 2.5), DMAc (≥ 99.8%) and polyethylene oxide (PEO: $M_v \approx 400{,}000$) were purchased from Sigma Aldrich Co. and used as received. Acetone (≥ 99.8%) was purchased from Biosolve Chimie Co. and used as received. The synthesis of Azo-Cel was reported in our previous paper.[20]

Electrospinning: Electrospinning was carried out by using a Fuence 'Esprayer ES-2000S2A' apparatus at room temperature (ca. 25 °C) and humidity (ca. 30%). The electrospun products were collected on two different types of metallic electrodes, namely a flat plate (20 cm × 20 cm) and a cylinder-shaped rotating drum (diameter: 10 cm; length: 15 cm) covered with Al foil. The electrodes are placed 15 cm below the tip of needle electrodes (Nordson stainless steel tips 18 GA (inner diameter = 0.84 mm) or 20 GA (inner diameter = 0.61 mm)). A high electric field (20-25 kV) was applied between the electrodes to draw polymer threads from the tip of the needle where polymer solutions were fed at various solution feed rates (6.0-

16.7 µL min^{-1}). The cylinder-shaped drum electrode was rotated at 1500 rpm to fabricate unidirectionally-aligned polymer fibers and their fabrics.

Preparation of Self-standing Azo-Cel and CA Fabrics: For the preparation of the self-standing Azo-Cel fabric, 10 mL of a PEO solution (4.5 wt% in deionized water) was first electrospun using a 20 GA needle under a 20 kV electric field at a 16.7 µL min^{-1} solution feed rate on a rotating drum electrode covered with Al foil. Then, 6 mL of an Azo-Cel solution (17 wt% in acetone/DMAc = 3/2 (v/v)) was electrospun on the same Al foil coated with the PEO textile using a 18 GA needle under 25 kV at 10 µL min^{-1} solution feed rate. Afterwards, the Al foil coated with the double-layered "Azo-Cel on PEO" textile was removed from the drum electrode and cut into small pieces. The specimen was then immersed in deionized water, which is a good solvent of PEO but a nonsolvent of Azo-Cel, to solubilize the PEO layer and detach the Azo-Cel layer from the Al foil without any physical pressure on the textile. After half a day, the PEO layer was completely dissolved and the Azo-Cel layer was detached from the Al foil as a floating textile that was dried under vacuum at 70 °C overnight to obtain a self-standing Azo-Cel fabric. For the preparation of the CA fabric, CA was directly electrospun onto an Al foil because the electrospun CA textile did not strongly adhere to the Al foil and was easily detachable from the foil without damaging it. Hence, 6 mL of a CA solution (17 wt% in acetone/DMAc = 2/1 (v/v)) was electrospun using a 20 GA needle under 20 kV at 10 µL min^{-1} solution feed rate on a rotating drum electrode covered with Al foil. The Al foil coated with CA textile was removed from the drum electrode and cut into small pieces. The CA textile was carefully peeled-off from the Al foil using tweezers to obtain a self-standing CA fabric.

ATR-FTIR Spectroscopy: The ATR-FTIR spectra were obtained using a PerkinElmer 'Spectrum Two' spectrometer. For the measurement of the self-standing Azo-Cel fabric, the sample was placed in such a way that the surface of the fabric where the PEO layer was attached (before the solubilization process) and the ATR crystal faced each other.

SEM: The electrospun products on Al foil were characterized using a FEI 'QUANTA FEG 250' SEM apparatus operating at an accelerating voltage of 2.5 kV. The specimens were coated with a ca. 4 nm thick layer of gold/palladium (Au/Pd) prior to the SEM observations. The diameters of the fibers in the textile and their distributions were statistically analyzed for 100 randomly selected fibers from the SEM images by using ImageJ open-source software. The thickness of the self-standing Azo-Cel fabric (ca. 40 μm) was estimated from the SEM image shown in Figure S1 (see supporting information).

WCA Measurement: The WCA of the Azo-Cel fabric was measured using an I.T. Concept 'Tracker' tensiometer at room temperature. The general procedure was as follows: a 5 μL of deionized water was dropped on a piece of Azo-Cel fabric fixed on a glass slide using double-sided tape and the contact angle was measured when the angle became stable after 90 seconds. After the measurement, the water droplet was sucked out from the specimen with tissue paper (Kimberly Clark 'Kimwipes'). Then, the specimen was irradiated with UV light (λ = 355 to 375 nm) using a SPOT UV Hamamatsu LC8 L9588 Hg-Xe lamp equipped with an A9616-07 filter at a light intensity of 60 mW cm^{-2} for 15 min in a darkened room. After the UV irradiation, the WCA was measured in the same manner as described above in a dark room. The water droplet was then sucked out, and a white fluorescent room light was turned on and the specimen was left for 30 mins under visible light before measuring the WCA again. The above-mentioned process was repeated over 5 cycles for 4 different pieces of Azo-Cel fabrics.

Photo-actuation Analysis: Three pieces of the self-standing Azo-Cel fabric (4 mm × 20 mm with the long side of the rectangle parallel to the principal axis of the aligned fibers) were anchored with tweezers and placed at three different distances away from the UV light (λ = 280 to 400 nm) source (Ushio UXM-200H, Hg/Xe 200W lamp equipped with a LOT-ORIEL 66216 dichroic mirror and a 59060 IR blocking filter), i.e., at 1, 2, and 4 cm, leading to different surface light intensities of 60, 45, and 25 mW cm^{-2}, respectively. The fabrics were irradiated by

the UV light in a darkened room for 30 minutes and were monitored using a Fujifilm X30 digital camera. The UV-induced photo-actuation behavior (angular movement) of the fabrics was characterized by measuring the difference between the angle of the UV-irradiated fabrics and the initial angle of the non-irradiated fabrics using a printed protractor sheet placed behind the specimens. A piece of the self-standing CA fabric (4 mm × 20 mm) anchored with tweezers was placed at 2 cm away from the UV light (the light intensity = 45 mW cm^{-2}) and monitored in the same manner.

Supporting Information

Supporting Information is available from the Wiley Online Library or from the author.

Acknowledgements

This study was financially supported by the France-Canada Research Fund (New Scientific Collaboration Support Program 2019), the Institut Carnot PolyNat (ANR-16-CARN-0025-0), and the Centre de Recherches sur les Macromolécules Végétales (CERMAV, CNRS). The authors acknowledge the support of Dr. C. Lancelon-Pin for the SEM observations at the Electronic Microscopy Platform (PMIEL) of the Institut de Chimie Moléculaire de Grenoble (ICMG), Ms. S. Ortega Murillo for the WCA measurements at CERMAV, Dr. K. Gorgy and Ms. A. Le-Pellec for the photo-actuation analysis at Département de la Chimie Moléculaire (DCM)/NanoBio laboratory. The authors are thankful to Prof. R. Pecora (Stanford University) for helpful suggestions during the writing of this manuscript.

Conflict of Interest

The authors declare no conflict of interest.

Received: ((will be filled in by the editorial staff))
Revised: ((will be filled in by the editorial staff))
Published online: ((will be filled in by the editorial staff))

References

[1] L. De Sio, B. Ding, M. Focsan, K. Kogermann, P. Pascoal-Faria, F. Petronela, G. Mitchell, E. Zussman, F. Pierini, *Chemistry – A European Journal* **2021**, 27, 6112.
[2] N. Bhardwaj, S. C. Kundu, *Biotechnology Advances* **2010**, 28, 325.
[3] A. Greiner, J. H. Wendorff, *Angew Chem Int Ed Engl* **2007**, 46, 5670.
[4] D. Li, Y. Xia, *Advanced Materials* **2004**, 16, 1151.
[5] Z.-M. Huang, Y. Z. Zhang, M. Kotaki, S. Ramakrishna, *Composites Science and Technology* **2003**, 63, 2223.
[6] B. Isaac, R. M. Taylor, K. Reifsnider, *Fibers* **2021**, 9, 4.
[7] J. Lee, Y. Deng, *Macromolecular Research* **2012**, 20, 76.
[8] S. Shang, F. Yang, X. Cheng, X. F. Walboomers, J. A. Jansen, *European cells & materials* **2010**, 19, 180.
[9] J. D. Schiffman, C. L. Schauer, *Polymer Reviews* **2008**, 48, 317.
[10] R. Sridhar, R. Lakshminarayanan, K. Madhaiyan, V. Amutha Barathi, K. H. C. Lim, S. Ramakrishna, *Chemical Society Reviews* **2015**, 44, 790.
[11] V. V. T. Padil, J. Y. Cheong, A. Kp, P. Makvandi, E. N. Zare, R. Torres-Mendieta, S. Wacławek, M. Černík, I.-D. Kim, R. S. Varma, *Carbohydrate Polymers* **2020**, 247, 116705.
[12] A. Memic, T. Abudula, H. S. Mohammed, K. Joshi Navare, T. Colombani, S. A. Bencherif, *ACS Applied Bio Materials* **2019**, 2, 952.
[13] D. Poshina, I. Otsuka, *Textiles* **2021**, 1, 152.
[14] Q. Zhu, S. Liu, J. Sun, J. Liu, C. J. Kirubaharan, H. Chen, W. Xu, Q. Wang, *Carbohydrate Polymers* **2020**, 235, 115933.
[15] A. Toncheva, F. Khelifa, Y. Paint, M. Voué, P. Lambert, P. Dubois, J.-M. Raquez, *ACS Applied Materials & Interfaces* **2018**, 10, 29933.
[16] J. Kim, S. Yun, Z. Ounaies, *Macromolecules* **2006**, 39, 4202.
[17] X. Qiu, S. Hu, *Materials* **2013**, 6, 738.
[18] H. Sehaqui, S. Morimune, T. Nishino, L. A. Berglund, *Biomacromolecules* **2012**, 13, 3661.
[19] I. Otsuka, K. Pandey, H. Ahmadi-Nohadani, S. Nono-Tagne, *ACS Macro Letters* **2021**, 10, 921.
[20] I. Otsuka, C. J. Barrett, *Cellulose* **2019**, 26, 6903.
[21] O. Bertrand, J.-F. Gohy, *Polymer Chemistry* **2017**, 8, 52.
[22] F. Ercole, T. P. Davis, R. A. Evans, *Polym. Chem.* **2010**, 1, 37.
[23] W. Du, X. Liu, L. Liu, J. W. Y. Lam, B. Z. Tang, *ACS Applied Polymer Materials* **2021**, 3, 2290.
[24] H. Yu, *Journal of Materials Chemistry C* **2014**, 2, 3047.
[25] O. S. Bushuyev, M. Aizawa, A. Shishido, C. J. Barrett, *Macromol Rapid Commun* **2018**, 39, 1700253.
[26] X. Pang, J.-a. Lv, C. Zhu, L. Qin, Y. Yu, *Advanced Materials* **2019**, 31, 1904224.
[27] T. Ikeda, M. Nakano, Y. Yu, O. Tsutsumi, A. Kanazawa, *Advanced Materials* **2003**, 15, 201.
[28] Y. Yu, M. Nakano, T. Ikeda, *Nature* **2003**, 425, 145.
[29] H. Finkelmann, E. Nishikawa, G. G. Pereira, M. Warner, *Physical Review Letters* **2001**, 87, 015501.
[30] C. L. van Oosten, C. W. M. Bastiaansen, D. J. Broer, *Nature Materials* **2009**, 8, 677.
[31] S. Iamsaard, S. J. Aßhoff, B. Matt, T. Kudernac, J. J. L. M. Cornelissen, S. P. Fletcher, N. Katsonis, *Nature Chemistry* **2014**, 6, 229.
[32] T. J. White, N. V. Tabiryan, S. V. Serak, U. A. Hrozhyk, V. P. Tondiglia, H. Koerner, R. A. Vaia, T. J. Bunning, *Soft Matter* **2008**, 4, 1796.

[33] S. Li, Y. Tu, H. Bai, Y. Hibi, L. W. Wiesner, W. Pan, K. Wang, E. P. Giannelis, R. F. Shepherd, *Macromolecular Rapid Communications* **2019**, 40, 1800815.
[34] P. Zhang, Z. Lan, J. Wei, Y. Yu, *ACS Macro Letters* **2021**, 10, 469.
[35] S. Sun, S. Liang, W.-C. Xu, G. Xu, S. Wu, *Polymer Chemistry* **2019**, 10, 4389.
[36] C. Fryer, M. Scharnagl, C. Helms, *AIP Advances* **2018**, 8, 065023.
[37] S. Wang, Y. Song, L. Jiang, *Journal of Photochemistry and Photobiology C: Photochemistry Reviews* **2007**, 8, 18.
[38] L. M. Siewierski, W. J. Brittain, S. Petrash, M. D. Foster, *Langmuir* **1996**, 12, 5838.
[39] N. Delorme, J. F. Bardeau, A. Bulou, F. Poncin-Epaillard, *Langmuir* **2005**, 21, 12278.
[40] L. F. V. Pinto, S. Kundu, P. Brogueira, C. Cruz, S. N. Fernandes, A. Aluculesei, M. H. Godinho, *Langmuir* **2011**, 27, 6330.
[41] Y. Huang, H. Kang, G. Li, C. Wang, Y. Huang, R. Liu, *RSC Advances* **2013**, 3, 15909.

The table of contents entry

An electrospun self-standing fabric consisting of a reversible molecular photo-switch, azobenzene, and a natural robust polysaccharide, cellulose, exhibits light-driven wettability changes and asymmetric deformations in response to alternate irradiation with UV and visible light to induce geometric deformation of the azobenzene moiety between the *trans* and *cis* isomers, which indicates a great potential for practical applications as novel photo-actuators.

Hamed Ahmadi-Nohadani, Steve Nono-Tagne, Christopher J. Barrett, and Issei Otsuka*

Electrospun Azo-Cellulose Fabric: A Smart Polysaccharidic Photo-actuator

ToC figure

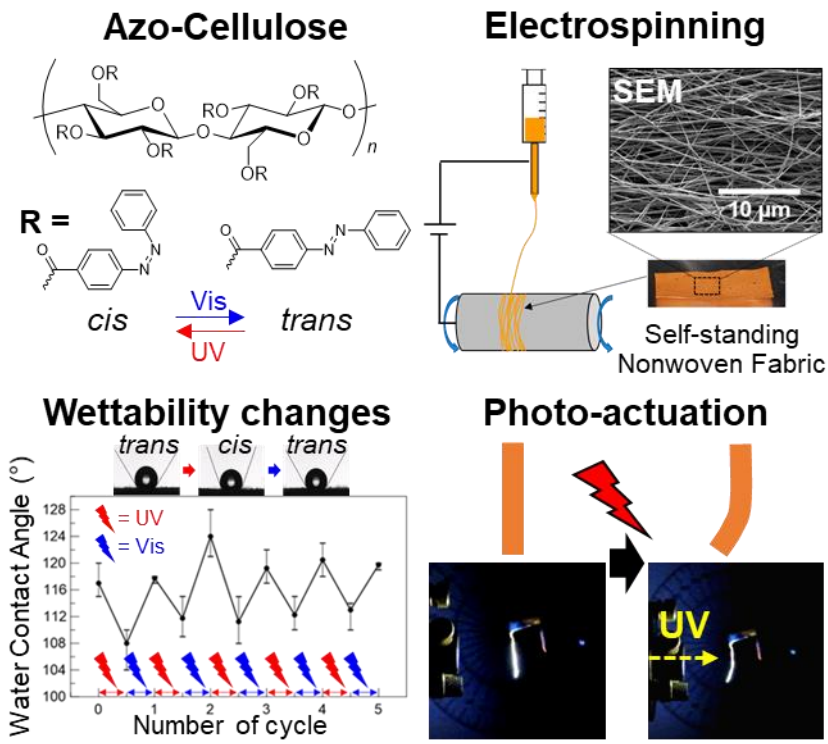

Supporting Information

Electrospun Azo-Cellulose Fabric: A Smart Polysaccharidic Photo-actuator

Hamed Ahmadi-Nohadani,[1] Steve Nono-Tagne,[1] Christopher J. Barrett,[2] and Issei Otsuka[*,1]*

[1] Université Grenoble Alpes, CNRS, CERMAV, Grenoble 38000, France

[2] Department of Chemistry, McGill University, Montreal H3A 0B8, Canada

[*]Corresponding author (I.O.)

Tel.: +33-4-76-03-76-82; *E-mail address*: issei.otsuka@cermav.cnrs.fr

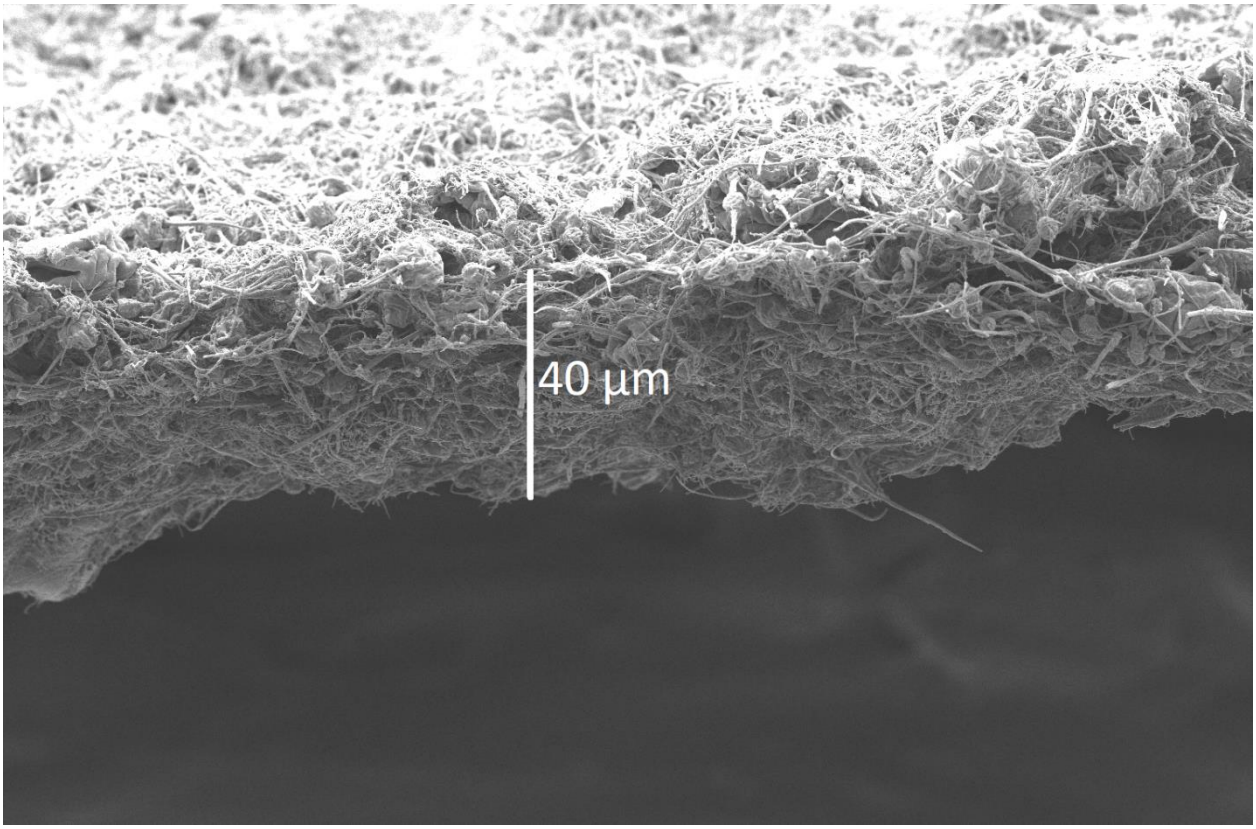

Figure S1. A SEM image of the self-standing Azo-Cel fabric (scale bar = 40 μm).

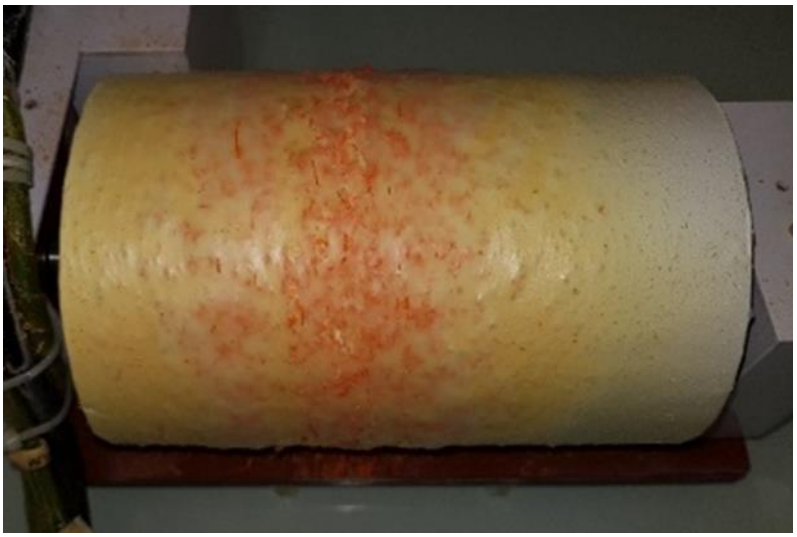

Figure S2. A picture of the co-electrospun product from the mixture of CA and azobenzene (molar ratio: glucose unit of CA/azobenzene = 1/3) in acetone/DMAc = 2/1 (v/v) (concentration of CA: 17 wt%) collected on the cylinder-shaped drum electrode.